



ELSEVIER

Available online at www.sciencedirect.com

SCIENCE @ DIRECT®

Journal of Hydrology xx (0000) xxx–xxx

 Journal
of
Hydrology

www.elsevier.com/locate/jhydrol

Multi-objective parameter estimation for simulating canopy transpiration in forested watersheds

D. Scott Mackay^{a,*}, Sudeep Samanta^a, Ramakrishna R. Nemani^b, Lawrence E. Band^c

^a*Department of Forest Ecology and Management, Institute for Environmental Studies, University of Wisconsin—Madison, 1630 Linden Drive, Madison, WI 53706, USA*

^b*School of Forestry, University of Montana, Missoula, MT 59812, USA*

^c*Department of Geography, University of North Carolina—Chapel Hill, Chapel Hill, NC 27514, USA*

Received 4 October 2001; accepted 13 March 2003

Abstract

A Jarvis based [Philos. Trans. R. Soc. London, Ser. B 273 (1976) 593] model of canopy stomatal conductance was evaluated in context of its application to simulating transpiration in a conifer forest covered watershed in the Central Sierra Nevada of California, USA. Parameters influencing stomatal conductance were assigned values using Monte Carlo sampling. Model calibration was conducted by evaluating predicted latent heat fluxes against thermal remote sensing estimates of surface temperature. A fuzzy logic approach was used to select or reject simulations and form a restricted set of ensemble parameter solutions. Parameter estimates derived from the ensembles were evaluated using theory on how stomatal conductance regulates leaf water potential to prevent runaway cavitation. Canopy level parameters were found to be sufficient for predicting hydraulically consistent transpiration when soils were well watered. A rooting length parameter controlling the amount of plant available water was a sufficient addition to the parameter set to predict hydraulically consistent transpiration when soil moisture stress was occurring. Variations in maximum stomatal conductance among different hillslopes within the watershed were explained by a light threshold parameter. The results demonstrate that the Jarvis model can be reliably parameterized using thermal remote sensing data for estimating transpiration in meso-scale watersheds.

© 2003 Published by Elsevier Science B.V.

Keywords: Stomatal conductance; Simulation model; Parameter estimation; Transpiration; Thermal remote sensing

1. Introduction

Spatially variable transpiration is a major component flux simulated by distributed land surface process models. Although there is a scarcity of observational data to directly support large-scale

simulation of canopy transpiration from forests, many models operating from watersheds to global scales (Running and Coughlan, 1988; Aber and Federer, 1992; Band et al., 1993; Running and Hunt, 1993; Famiglietti and Wood, 1994; Wigmosta et al., 1994; Vertessy et al., 1996; Foley et al., 1996, 2000; Mackay and Band, 1997; Sellers et al., 1997; and others) simulate transpiration using some form of the Penman–Monteith combination equation (P–M) (Monteith, 1965) and one of several empirical models

* Corresponding author. Tel.: +1-608-262-1669; fax: +1-608-262-9922.

E-mail address: dsmackay@facstaff.wisc.edu (D.S. Mackay).

of stomatal conductance (Jarvis, 1976; Lohammar et al., 1980; Ball et al., 1987). Although there are numerous sources of uncertainty in P–M models, the unknowns associated with stomatal conductance are most critical for understanding vegetation responses to climate change and land use pressures. Mackay et al. (2003) show that Jarvis-type models mimic the stomatal regulation of leaf water potentials in a detailed canopy model operating at sub-daily time resolution, with in situ micrometeorological measurements and sap flux data for calibration. The study by Mackay et al. (2003) was limited to four forest stands each approximately 30 m in diameter. To extend the applicability of their approach to watershed or global scales necessitates finding tractable data sources and more moderate model detail.

One potential source of data for characterizing the state of a land surface is thermal remote sensing. Thermal remote sensing data is a measure of surface temperature, which is a function of energy partitioning and surface resistance. Foliage temperature has been shown to relate to soil moisture, plant moisture stress, and transpiration (Idso et al., 1978; Jackson et al., 1981). This has led to numerous applications of thermal remote sensing to study canopy processes (Goward et al., 1985; Pierce and Congalton, 1988; Holbo and Luvall, 1989; Nemani and Running, 1989; Kustas et al., 1994; Carlson et al., 1995; Anderson et al., 1997; Franks and Beven, 1997; Bastiaanssen et al., 1998; Norman et al., 2000). These methods have been successful using very different approaches. Representative approaches include modeling with detailed ground flux measurements and sub-daily remote sensing measurements to look at thermal inertia (Anderson et al., 1997; Norman et al., 2000), limiting the analysis to large-scale remote sensing with strong moisture gradients and well-coupled forest canopies (Nemani and Running, 1989), or calibrating a model using Monte Carlo analysis with contrasting vegetation types (Franks and Beven, 1997).

In this paper, the latter two approaches are combined to evaluate a Jarvis-type model as used within the Regional Hydro-Ecological Simulation System (RHESSys) (Band et al., 1993) applied to a meso-scale watershed in the Central Sierra Nevada. RHESSys has been and continues to be applied successfully in numerous forested watershed studies

(Band et al., 1996; Creed et al., 1996; Watson et al., 1996; Mackay and Band, 1997; White et al., 1998; Baron et al., 2000; Tague and Band, 2001; Zhu and Mackay, 2001; Mackay, 2003; Samanta and Mackay, 2003). Its ability to predict stream flow, nitrate export, and responses to forest manipulation and road construction are documented in these studies. However, neither RHESSys nor any model like it has been tested for consistent spatial transpiration. The question is whether RHESSys can produce transpiration at a watershed scale that is consistent with plant water relation theory. Significant progress has recently been made in the understanding of hydraulic limitations to canopy transpiration. These limitations have helped in constraining parameters for a Jarvis-type model at the stand level (Mackay et al., 2003). It is hypothesized that transpiration estimates can be similarly evaluated through calibration of Jarvis-type parameters controlling stomatal conductance at larger spatial scales and on daily time-step, by comparing model predictions and thermal remote sensing estimates of surface energy partitioning. Rejecting this hypothesis would mean that the model is either deficient with respect to processes such as soil water distribution, the Jarvis-type model is a poor approximation to the stomatal conductance at daily time-steps or at larger spatial scales, or the combination of data and models used in the analysis are insufficient to resolve the underlying regulation of leaf water potential by stomata, which ultimately affects energy partitioning.

The paper is organized as follows. First, a summary of the most relevant elements of plant water relations are presented to build a framework for relating the Jarvis-type stomatal conductance model to tree hydraulic theory. This is followed by the methods, which describes an automated calibration based on Samanta and Mackay (2003) and restricted using the tree hydraulic theory (Mackay et al., 2003). Relevant details on RHESSys are presented, followed by the analysis of thermal remote sensing imagery, results, discussion, and conclusions.

2. Plant water relations and the Jarvis model of stomatal conductance

Canopy transpiration from forests is generally simulated with the well-known P–M ‘big leaf’ model

(Monteith, 1965). A key variable in P–M is canopy conductance, which is determined by the product of stomatal conductance, g_s and leaf area, L . Models of stomatal conductance address one or more environmental (extrinsic) and physiological (intrinsic) conditions of the leaf stomata. There are two distinct empirical models of stomatal conductance: Ball–Berry (Ball et al., 1987; Leuning et al., 1995) and Jarvis (Jarvis, 1976; Lohammar et al., 1980). The Ball–Berry model emphasizes the rate of carbon assimilation in controlling stomatal conductance, but places little emphasis on water supply and demand. Jarvis models more directly address water supply and demand through soil water limitation and atmospheric vapor pressure deficit functions, respectively. Jarvis-type models have the general form:

$$g_s = g_{S_{\max}} \prod f_i, \quad (1)$$

where $g_{S_{\max}}$ is a theoretical maximum stomatal conductance under assumed optimal environment and leaf conditions. A series of multiplicative functions of environmental factors (f_i) are applied to reduce actual leaf level stomatal conductance from the theoretical maximum level. Typically, one function considers the stomatal sensitivity, δ , to atmospheric vapor pressure deficit, D . The $g_{S_{\max}}$ parameter can vary widely among and within species (Kelliher et al., 1995; Ewers et al., 2001) and δ is widely believed to increase with maximum stomatal conductance (Jarvis, 1976, 1980; McNaughton and Jarvis, 1991; Monteith, 1995; Saliendra et al., 1995; Oren et al., 1999). Low vapor pressure gradient conditions favor stomatal control by assimilation rate, but as D increases stomata close to reduce water loss (Ball et al., 1987; Monteith, 1995; Saliendra et al., 1995; Yong et al., 1997). One advantage of the Jarvis model for water flux estimates is that it directly addresses plant response to D . This suggests that it operates best when the rate of water loss is high and, hence, hydrologically significant. Furthermore, recent developments in plant hydraulic theory have been successfully combined with Jarvis models (Oren et al., 1999; Ewers et al., 2000) and tested in diurnal canopy models on a range of forest species (Mackay et al., 2003).

Eq. (1) is a proxy for the hydraulic functioning of the soil–plant–atmosphere continuum. In the absence

of stomatal control, a high rate of water loss from a plant leads to a rapid decline in leaf water potential. This increases the risk of hydraulic failure in the plant (Sperry et al., 1998; Oren et al., 1999; Ewers et al., 2000). The relationship between stomatal conductance and water potential can be expressed with the steady-state assumption and Darcy's law (Tyree and Ewers, 1991; Ewers et al., 2000):

$$G_s = K_L/D(\Psi_S - \Psi_L - h\rho_w g), \quad (2)$$

where G_s is canopy average leaf level stomatal conductance, K_L is leaf-specific whole-plant hydraulic conductance, Ψ_S and Ψ_L are bulk soil and leaf water potentials, respectively, and $h\rho_w g$ is the gravitational potential for a plant of height h . K_L declines with water potential due to soil drying, cavitation in the xylem, and other factors. As K_L declines a further drop in water potential is needed to sustain increasing E_C per unit leaf area (L). This drop in water potential further reduces K_L as a positive feedback. Once the maximum safe transpiration rate is exceeded then runaway cavitation ensues. Runaway cavitation refers to K_L being driven to zero causing hydraulic failure and possible plant mortality (Tyree and Sperry, 1988). Eq. (2) also captures the well-known fact that G_s is inversely proportional to D (Jarvis, 1976; McNaughton and Jarvis, 1991), which drives down stomatal conductance even when plants are well watered in the soil. This is shown conceptually in Fig. 1. G_s is further shown to be sensitive to increasing D in proportion to some maximum conductance, $g_{S_{\max}}$, or its proxy (Oren et al., 1999):

$$G_s = G_{S_{\text{ref}}} - m \ln D, \quad (3)$$

where $G_{S_{\text{ref}}}$ is a substitute for $g_{S_{\max}}$ defined at $D = 1$ kPa and $m = dG_s/d \ln D$ is the sensitivity of stomatal conductance to increasing D . In Eq. (3), $G_{S_{\text{ref}}}$ is typically near linearly related to the sensitivity of stomatal conductance to D . Based on a large amount of porometry and sap flux data, Oren et al. (1999) have shown that $m \approx 0.6G_{S_{\text{ref}}}$ applies universally to all species whose stomata regulate leaf water potential to just prevent runaway cavitation.

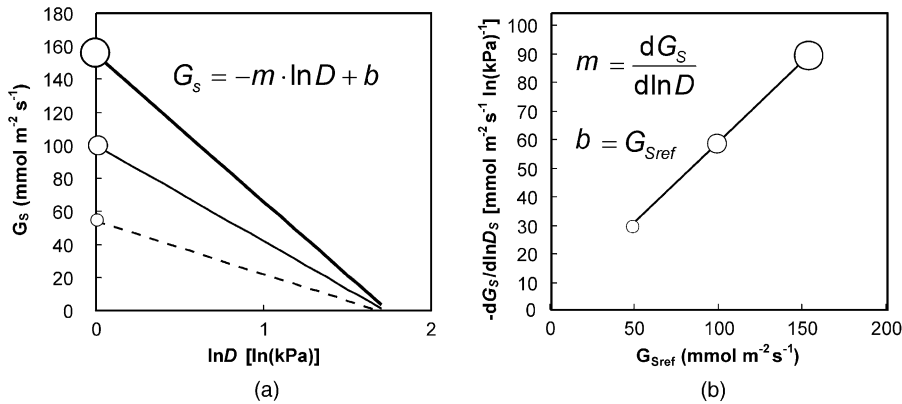


Fig. 1. The rates of stomatal closure (lines) in response to vapor pressure deficit are proportional to the maximum stomatal conductances (circles) (a), have been shown to result in all species that just regulate leaf water potential to prevent runaway cavitation to lie along a line representing the stomatal sensitivity to vapor pressure deficit versus reference conductance at 1 kPa ($\ln D = 0$).

3. Methods

3.1. Overview of the model parameterization approach

In this paper, two distinct stages of parameter estimation are used. The first stage of parameter estimation follows a traditional automated calibration. Many simulations are run in which parameters affecting stomatal conductance are assigned values using Monte Carlo sampling. Each simulation result is then evaluated by applying a linear least-squares regression between simulated evaporative fraction from RHESSys and surface temperature from thermal remote sensing data. For each least-squares regression, the coefficient of determination (or R^2) is calculated. The R^2 is then considered a fuzzy measure of the goodness-of-fit for its respective simulation result. The set of R^2 measures for all simulations is considered a fuzzy set (Samanta and Mackay, 2003). An information-theoretic tool is then applied to the fuzzy set to form a restricted set in which only ‘good’ simulations retained. A restricted set is used as an ensemble solution in the second stage of parameter estimation. A separate ensemble solution is produced for each areal unit simulated by RHESSys, and in the present work these areal units are hillslopes.

The second stage of parameter estimation applies the universal line represented by Eq. (3) and shown in Fig. 1. For each ensemble δ is related to g_{Smax} . When a δ/g_{Smax} combination falls on the universal line, it is

assumed to be consistent with plant hydraulic theory. Otherwise, it is considered inconsistent with the theory. To be consistent with the conventions of Oren et al. (1999), Jarvis parameters (δ and g_{Smax}) are mapped into their respective universal line counterparts (m and G_{Sref}). For the remainder of this paper the use of δ and g_{Smax} will be restricted to discussion of model function, not plant physiology. Discussion of plant physiology will use m and G_{Sref} .

3.2. Stage 1: model-independent automated parameterization

An objective automated parameter estimation framework (Samanta and Mackay, 2003) was used to calibrate RHESSys. The approach is based on a number of hydrologic parameter estimation schemes (Kuczera, 1982, 1983; Sorooshian and Gupta, 1983; Spear and Hornberger, 1990; van Stratten and Keesman, 1991; Klepper et al., 1991; Binley and Beven, 1991; Melching, 1995; Kuczera and Parent, 1998; Gupta et al., 1998; Yapo et al., 1998; Boyle et al., 2000). It combines Monte Carlo sampling and measures of uncertainty derived from information processing. One information-theoretic expression of uncertainty in information processing is the Hartley (1928) Function:

$$H(A) = \log_2 |A|, \quad (4)$$

where $H(A)$ is the Hartley Function for a finite set, A , and $|A|$ is its cardinality. Eq. (4) is a measure of

385 the non-specificity arising from an inability to identify
 386 a unique solution. Higher values of $H(A)$ represent
 387 greater non-specificity. If A represents a set of
 388 retained simulations, each defined by a simulation
 389 model and its parameters, then $H(A)$ is the non-
 390 specificity associated with this equifinal (Beven and
 391 Binley, 1992) set of simulations.

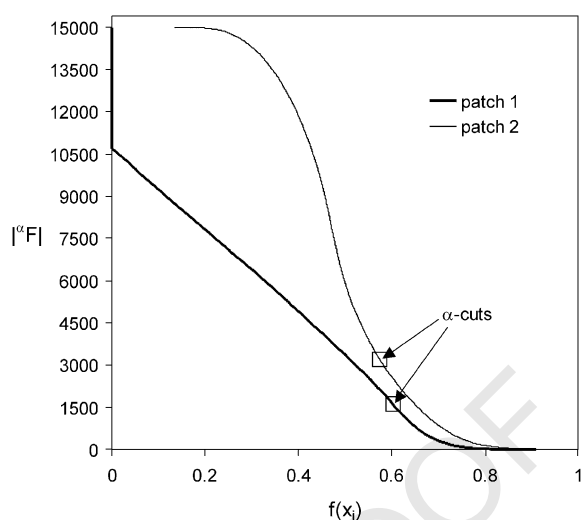
392 The above notion of the non-specificity of a set of
 393 simulations can be extended to incorporate measures
 394 of model fitness. If each simulation has an associated
 395 measure of fitness or degree of fit to some observation
 396 data, then the acceptable set of models can be
 397 considered a fuzzy set (Zadeh, 1965). For a fuzzy
 398 set, F , defined by a measurement of fitness, $f(x_i)$, for
 399 member x_i within the domain, X , of all simulations, a
 400 fuzzy logic measure of the non-specificity of F is
 401 (Higashi and Klir, 1982; Klir and Wierman, 1998):

$$402 \quad U(F) = \int_0^{h(F)} \log_2 |\alpha F| d\alpha + (1 - h(F)) \log_2 |X|, \quad (5)$$

403 where $U(F)$ is the U -uncertainty associated with F ,
 404 $|\alpha F|$ is the cardinality of an α -cut of F (i.e. the number
 405 of members that remain in the set if all members with
 406 a degree of fitness less than α are removed from F),
 407 $h(F)$ is the height of F (or maximum degree of fitness
 408 in F), and $|X|$ is the cardinality of the universal set (i.e.
 409 the population of simulations). A discrete approxi-
 410 mation of Eq. (5) is given by

$$411 \quad U(r) = \sum_{i=2}^n (r_i - r_{i+1}) \log_2 i + (1 - r_1) \log_2 n, \quad (6)$$

412 where r is the ordered possibility distribution (Zadeh,
 413 1978) derived from the fuzzy set F and r_{n+1} is
 414 assumed to be 0. Fig. 2 shows two typical possibility
 415 distributions relating $f(x_i)$, which is the goodness-of-
 416 fit measure, and $|\alpha F|$, as well as the physical meaning
 417 of the α -cut. Both distributions are shown to have an
 418 α -cut of about 0.6, at which they yield very different
 419 cardinalities. Relations that are skewed towards the
 420 low end, and thus have only a few high $f(x_i)$ models,
 421 are better than relations having too many high $f(x_i)$
 422 values. The ideal distribution of simulations relation
 423 has one with $f(x_i) = 1.0$ and all others with $f(x_i) =$
 424 0.0 . This would represent a case where the best
 425 simulation is uniquely identifiable. For numerous
 426 reasons, including model flaws, parameter trade-offs,
 427 and limitations of objective functions, hydrologic



433
 434
 435
 436
 437
 438
 439
 440
 441
 442
 443
 444
 445
 446
 447
 448
 449
 450
 451
 452
 453
 454
 455
 456
 457
 458
 459
 460
 461
 462
 463
 464
 465
 466
 467
 468
 469
 470
 471
 472
 473
 474
 475
 476
 477
 478
 479
 480

Fig. 2. Shown is an illustration of the types of possibility distributions that are commonly obtained from the U -uncertainty analysis. The plots represent the relationship between cardinality on the y-axis and value returned by some model evaluation objective function applied to simulations of two hypothetical landscape patches. Shown are the α -cuts obtained by minimizing $|U(r) - \log_2 k|$. It is important to note that similar α -cuts may be obtained from different sets of simulations in which the retained model sets have very different cardinalities.

models do not satisfy this ideal (Oreskes et al., 1994; Mackay and Robinson, 2000).

It is tempting to set the α -cut at such a level that only one simulation is retained. This is the traditional approach to model calibration. However, an objective criterion provides a better way to define the α -cut to form a restricted set from the fuzzy set (Samanta and Mackay, 2003). Initially, this α -cut should be selected with caution. On the one hand, useful information in the fuzzy set may be lost if an arbitrarily high α -cut is selected. An arbitrarily high α -cut may also admit a false sense of specificity to the identified model parameters. On the other hand, an arbitrarily low α -cut may include too many simulations of poor quality. Information Theory presents a rich set of tools for extracting the full information content of a fuzzy set. One tool, the Principle of Uncertainty Invariance (Klir and Wierman, 1998), transforms a fuzzy set into a ‘crisp’ restricted set that approximates the respective fuzzy set by virtue of having the same U -uncertainty. The α -cut is chosen at the k th element of the ordered possibility distribution at which $|U(r) - \log_2 k|$ is minimized. As an illustration, consider the ordered

481 fuzzy set $F = \{0.9, 0.8, 0.8, 0.7, 0.6, 0.4, 0.1, 0.1\}$. It is
 482 possible to calculate $|^\alpha F| = 4.4$ as the sum of fuzzy
 483 memberships in the set and $U(r) = 2.2$ as its
 484 associated U -uncertainty. The size of the restricted
 485 set is determined by equating the U -uncertainty of the
 486 fuzzy set (Eq. (6)) to the Hartley Function (Eq. (4)) for
 487 the desired crisp set. The value of k (5 in this example)
 488 is the required cardinality of the restricted set, which
 489 means that the top five elements in F are retained and
 490 the α -cut is placed at 0.6. An advantage of this
 491 approach is that the selection of the α -cut is not
 492 subject to interpretation or modification as the goals of
 493 a modeling exercise change. A disadvantage of the
 494 approach is that it does not consider intuition about
 495 the physical system, which is an essential part of
 496 parameter estimation (Boyle et al., 2000). However,
 497 once an objective solution set has been established,
 498 further analysis can be applied to determine if a more
 499 refined solution can be found. In this paper, a simple
 500 averaging of the respective parameter values from the
 501 restricted sets is tested by evaluating the degree to
 502 which the chosen parameters for a Jarvis-type model
 503 are consistent with the plant hydraulic theory
 504 relationships (Refer to Section 2). The Jarvis-type
 505 model and its parameterization are described in
 506 Section 3.3.

508 3.3. Stage 2: parameterization specific to RHESSys 509 canopy transpiration

511 RHESSys combines forest canopy gas exchange
 512 processes, soil moisture balance, and lateral saturated
 513 through flow (Band et al., 1993). It represents
 514 watersheds as collections of hillslopes, which are
 515 themselves divided into elevation zones for adiabatic
 516 adjustment of air temperature, T_a . Each elevation zone
 517 is segmented into hydrologically uniform patches
 518 defined using the TOPMODEL topography and soil
 519 index (TSI) (Beven and Kirkby, 1979; Beven, 1986;
 520 Sivapalan et al., 1987; Quinn et al., 1995). All vertical
 521 fluxes, including evapotranspiration, are calculated at
 522 the patch level. Complete details on the design and
 523 implementation of RHESSys are provided in previous
 524 publications (Band et al., 1993; Mackay and Band,
 525 1997; Mackay, 2003). This section focuses on model
 526 components that directly affect the calculation of
 527 stomatal conductance. Leaf level stomatal conduc-
 528 tance (m s^{-1}) is determined (from Eq. (1)) in

RHESSys as:

$$529 \quad g_S = g_{S_{\max}} g_1(D) g_2(\Psi_L) g_3(Q), \quad (7) \quad 530$$

531 where
 532

$$533 \quad g_1(D) = 1 - \delta D \quad (8) \quad 534$$

535 and δ [$(\text{kPa})^{-1}$] has been previously defined as the
 536 sensitivity of stomatal conductance to D . From the
 537 earlier discussion it should be apparent that Eq. (8) is a
 538 surrogate for stomatal response to the rate of water
 539 loss from the canopy, which is strongly related to D in
 540 well-ventilated forest canopies (McNaughton and
 541 Jarvis, 1991). This can be interpreted in the terms
 542 used in Eq. (4) by mapping $g_{S_{\max}}$ and δ into $G_{S_{\text{ref}}}$ and
 543 $dG_S/d \ln D$, respectively. The $g_{S_{\max}}$ parameter rep-
 544 resents a theoretical optimal stomatal conductance
 545 under ideal conditions (i.e. low D , sufficient light,
 546 moderate temperature, well-watered soils). Following
 547 Eq. (8) $g_S \equiv g_{S_{\max}}$ at $D = 0$ kPa. It is not possible to
 548 measure g_S at $D = 0$ kPa, and so $g_{S_{\max}}$ is transformed
 549 into $G_{S_{\text{ref}}}$ (at $D = 1$ kPa as defined by Oren et al.
 550 (1999)) as follows:

$$551 \quad G_{S_{\text{ref}}} = g_{S_{\max}} (1 - \delta). \quad (9) \quad 552$$

553 Similarly δ is converted into m as follows:

$$554 \quad m = dG_S/d \ln D = g_{S_{\max}} d\delta/d \ln D, \quad (10) \quad 555$$

556 in which the derivative is calculated by finite-
 557 difference at two values of D (Mackay et al., 2003).
 558 The other functions (g_2 and g_3) in Eq. (7) are not
 559 modified from their standard expressions. Stomatal
 560 conductance is further reduced using a hyperbolic
 561 function of leaf water potential, Ψ_L , which is assumed
 562 to be equal to pre-dawn soil water potential calculated
 563 using a van Ganuchten (1980) formulation parameter-
 564 ized using Brooks and Corey (1964) soil hydraulic
 565 parameters. Stomatal conductance is reduced linearly
 566 with the ratio of absorbed radiation in the canopy to a
 567 minimum threshold radiation, Q_{\min} .

568 RHESSys calculates soil water potential within a
 569 depth of soil defined by plant rooting length, R_L .
 570 R_L is varied spatially to account for two competing
 571 controls on water supply: (1) the tendency for
 572 capillarity to recharge a drying rooting zone when
 573 there is a shallow perched water table, and (2) the
 574 need for sufficient R_L to support the water demand
 575 associated with a given leaf area index, L (Grier
 576 and Running, 1977; Gholz, 1982), or, equivalently, 576

the root-shoot ratio. R_L is spatially co-varied with L and S (Mackay, 2003), expressed for a given patch, i , of uniform TSI within hillslope, h , as

$$R_{L,i} = R'_h L_{h,i} f_h(S_{h,i}), \quad (11)$$

where R'_h is intrinsic rooting length (per unit $L_{h,i}$) for a mesic site on h (m), $f_h(S_{h,i})$ is a function, which, through dimensional analysis, describes relative soil saturation deficit at i with respect to average soil saturation deficit within h , and $L_{h,i}$ is leaf area index defined at i on h ($\text{m}^2 \text{m}^{-2}$). Eq. (11) accounts for higher water demand environments (e.g. south-facing slopes, high temperatures) by increasing R'_h . Furthermore, high $L_{h,i}$ requires proportionally deeper roots to supply adequate water to the canopy. Sites with low saturation deficits do not require deep roots, and roots cannot survive long in a shallow water table (Larcher, 1995).

The derivation of $f_h(S_{h,i})$ is based on elements of TOPMODEL (Beven, 1986; Beven and Kirkby, 1979; Sivapalan et al., 1987). Profile saturation deficit is scaled from hillslope facet average saturation deficit as

$$\langle S_h \rangle - S_{h,i} = m_h (\text{TSI}_{h,i} - \langle \text{TSI}_h \rangle), \quad (12)$$

where $\langle S_h \rangle$ is mean saturation deficit for h (m), $S_{h,i}$ is saturation deficit of patch i of h (m), m_h is a parameter that describes the rate of decay of saturated hydraulic conductivity through a soil profile in hillslope h , $\text{TSI}_{h,i}$ is topography–soils index at patch i of hillslope h (m), and $\langle \text{TSI}_h \rangle$ is hillslope average topography–soils index (m). $\text{TSI}_{h,i}$ is calculated as follows:

$$\text{TSI}_{h,i} = \ln \left(\frac{a_{h,i} t_h}{t_{h,i} \tan \beta_{h,i}} \right), \quad (13)$$

where $a_{h,i}$ is accumulated upslope drainage area per unit contour width (m), $\beta_{h,i}$ is local topographic slope, $t_{h,i}$ is local soil transmissivity (m day^{-1}), and t_h is hillslope average transmissivity (m day^{-1}). Eq. (12) can be conditionally expanded to describe $S_{h,i}$ as

a function of $\langle S_h \rangle$:

$$S_{h,i} = \begin{cases} = \langle S_h \rangle, & \frac{\langle \text{TSI}_h \rangle}{\text{TSI}_{h,i}} = 1 \\ < \langle S_h \rangle, & \frac{\langle \text{TSI}_h \rangle}{\text{TSI}_{h,i}} < 1. \\ > \langle S_h \rangle, & \frac{\langle \text{TSI}_h \rangle}{\text{TSI}_{h,i}} > 1 \end{cases} \quad (14)$$

From Eq. (14) the relative saturation deficit can be determined from hillslope average conditions with the dimensionless form:

$$f_h(S_{h,i}) = \frac{\langle \text{TSI}_h \rangle}{\text{TSI}_{h,i}}. \quad (15)$$

Substituting Eq. (15) into Eq. (11) gives a relation for scaling rooting length along joint moisture and leaf area gradients within a hillslope,

$$R_{L,i} = R'_h L_{T_{h,i}} \frac{\langle \text{TSI}_h \rangle}{\text{TSI}_{h,i}}. \quad (16)$$

The parameter, R'_h , can be modified to linearly scale the volume of soil available for plant access to water.

3.4. Evaluation data set

Data to test the Jarvis-based model in RHESSys was obtained from the Onion Creek Experimental Forest, a 10 km² watershed located along the crest of the Central Sierra Nevada of Annual precipitation averages 1300 mm, of which 90% falls as snow between October 1 and March 31. Relief within the watershed is about 1000 m, with the highest elevation occurring at ca. 2600 m above mean sea level. Soils are generally poorly developed loamy sands overlying highly permeable rhyolitic ash and latite deposits (MacDonald, 1987). The soils and underlying parent material have a high storage capacity producing long lags in the baseflow recession (MacDonald, 1986). Vegetation cover is predominantly mature to old-growth mixed needle-leaf conifers. The dominant tree species in the basin are White Fir (*Abies concolor*), Red Fir (*Abies magnifica*), Sugar Pine (*Pinus lambertiana*), Jeffrey Pine (*Pinus jeffreyi*), Lodgepole Pine (*Pinus contorta*), and Incense Cedar (*Calocedrus decurrens*). Cedar generally occupies lower

673 elevations, pine at mid-elevations, and fir at higher
674 elevations.

675 Radiometric thermal data was acquired with the
676 NASA-Ames Research Center's airborne Thematic
677 Mapper Simulator (TMS), a Daedalus scanner flown
678 aboard a U-2 aircraft on July 2 and August 6, 1985.
679 The image data was collected in conjunction with
680 field-measured surface temperature and soil moisture
681 (Pierce and Congalton, 1988; MacDonald, 1989). On
682 July 2, soil moisture measurements in the watershed
683 showed soil moisture levels between field capacity
684 and saturation. On August 6 the soils were well below
685 field capacity and approaching wilting point in some
686 plots (MacDonald, 1989). The TMS images were
687 collected at approximately solar noon at a flying
688 height commensurate with a sensor resolution of 30 m
689 (or 0.09 ha per observation). The flight lines were
690 centered over Onion Creek to avoid off-nadir
691 geometry problems, allowing for relatively accurate
692 co-registration of the TMS with a Landsat Thematic
693 Mapper 4 (TM) scene (RMS error < 15 m). Sensor
694 radiance values, r , were converted to kinetic tem-
695 peratures, t , with the following regression and
696 parameters (Table 1) obtained from black-body
697 radiation sensor calibration reference plates, atmos-
698 pheric correction, and ground control within Onion
699 Creek (Pierce and Congalton, 1988):

$$T_s = \frac{t_{\max} - t_{\min}}{r_{\max} - r_{\min}}(10r - r_{\min}) + t_{\min}. \quad (17)$$

703 No adjustment was made for variations in surface
704 emissivity, as the range of cover types in Onion Creek
705 (occasional bare soil to predominantly dense conifer
706 canopy) should have emissivities of 0.9–0.95, which
707 translates into 1–3% error when inverting the Stefan–
708 Boltzmann Equation to convert from radiant to kinetic
709 temperature.

710 Kinetic temperatures are influenced by a number
711 of other factors in complex topography. These
712 factors include stomatal, boundary and aerodynamic

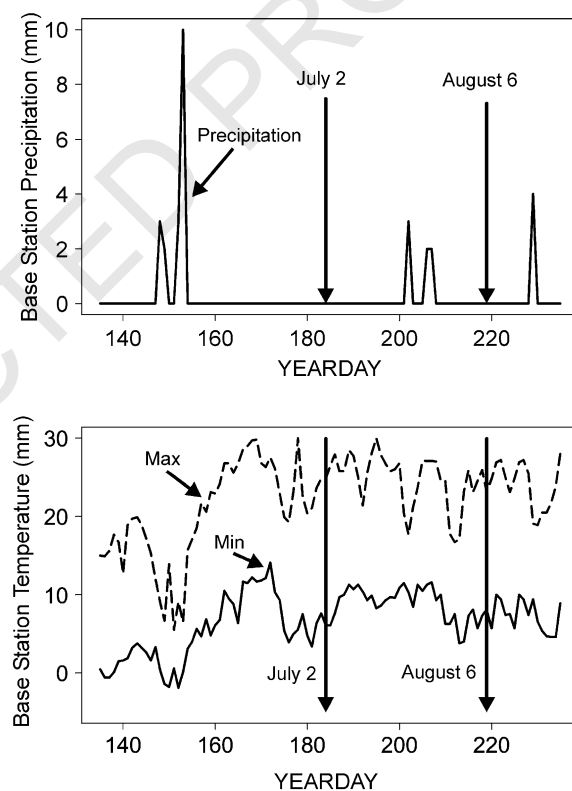
713 Table 1

714 Black body reference plate regression parameters used in Eq. (14) to
715 convert TMS pixel values to radiant temperatures

Date	t_{\max}	t_{\min}	r_{\max}	r_{\min}
July 2	32.21	8.18	149.00	105.00
August 6	32.32	8.49	150.00	110.00

720

721 resistances, which effect latent and sensible heat
722 transfer; meteorological differences, such as cloud
723 cover and air temperature between flight dates;
724 temperature lapse with elevation; land surface–sun
725 geometry; and forest canopy density. Meteorological
726 data was obtained from the Central Sierra Snow Lab.
727 Fig. 3 shows daily temperatures (maximum and
728 minimum) and precipitation for the period beginning
729 before the July 2 TMS scene and ending after the
730 August 6 scene. Both dates show similar daily high
731 and low temperatures, and clear skies following
732 several days with no precipitation. Aerodynamic
733 conductance was assumed high (set at 0.2 m s^{-1}) for
734 the dense, conifer needle-leaf forests covering much
735 of Onion Creek. TM data was used to derive leaf area
736 index (LAI) using ground-based calibration and
737 image processing procedures described in Nemani
738



739
740
741
742
743
744
745
746
747
748
749
750
751
752
753
754
755
756
757
758
759
760
761
762
763
764
765
766
767
768
769
770
771
772
773
774
775
776
777
778
779
780
781
782
783
784
785
786
787
788
789
790
791
792
793
794
795
796
797
798
799
800
801
802
803
804
805
806
807
808
809
810
811
812
813
814
815
816
817
818
819
820
821
822
823
824
825
826
827
828
829
830
831
832
833
834
835
836
837
838
839
840
841
842
843
844
845
846
847
848
849
850
851
852
853
854
855
856
857
858
859
860
861
862
863
864
865
866
867
868
869
870
871
872
873
874
875
876
877
878
879
880
881
882
883
884
885
886
887
888
889
890
891
892
893
894
895
896
897
898
899
900
901
902
903
904
905
906
907
908
909
910
911
912
913
914
915
916
917
918
919
920
921
922
923
924
925
926
927
928
929
930
931
932
933
934
935
936
937
938
939
940
941
942
943
944
945
946
947
948
949
950
951
952
953
954
955
956
957
958
959
960
961
962
963
964
965
966
967
968
969
970
971
972
973
974
975
976
977
978
979
980
981
982
983
984
985
986
987
988
989
990
991
992
993
994
995
996
997
998
999
1000

Fig. 3. This shows the meteorological conditions spanning the period around the two selected dates (July 2 and August 6) for the TMS imagery. Note that both dates occur during a dry period with no recent rainfall, and with similar maximum and minimum temperatures.

et al. (1993). A USGS 30 m digital elevation model (DEM) was used to identify hillslopes that account for variability in land surface–sun geometry, and elevation bands that account for temperature lapse rates. A digitized soils map was acquired from the US Forest Service, and used for soil parameterization of RHESSys. Table 2 summarizes topography, vegetation, and other hillslope facet mean properties of Onion Creek, partitioned into 25 hillslope partitions (Liang and Mackay, 2000).

A separate objective function was used for each TMS scene for each model. Linear least-squares regression between evaporative fraction, $\sigma = \lambda E_C / Q$, and surface departure from air temperature, $dT = T_s - T_a$ was used to evaluate model fitness. The reason for using σ is that it remains nearly constant during the mid-day period (Crago, 1996; Crago and Brutsaert, 1996) and so it is less likely to be sensitive

to short-term changes in micrometeorological conditions than is latent heat flux alone. Furthermore, whereas λE_C and Q both give a non-linear fit to surface temperature data due to their asymptotic response with leaf area index through the Beer–Lambert Equation, their ratio is close to linear. As a requirement for using TMS imagery collected at a single point in time at solar noon, it is necessary to assume that midday dT is correlated with daily E_C at a given aerodynamic conductance (Seguin and Itier, 1983; Carlson et al., 1995). Furthermore, it was assumed that soil heat flux had a minimal influence on canopy temperature given the high leaf area (Carlson et al., 1995). Finally, residuals derived from the best model for each hillslope facet for each TMS scene were checked for trends. There were no visible trends in the residuals that would suggest a linear fit was inappropriate.

Table 2

This shows a summary of the average properties of all hillslopes in the Onion Creek watershed partitioning. Number of zones refers to the number of elevation zones used to capture within-hillslope adiabatic temperature lapse rates. Each zone represents an increment of 30 m altitude, such that a hillslope with 20 zones has an elevation range of about 600 m

Hillslope identifier	Area (ha)	Aspect (°)	Elevation (m)	Slope (°)	L ($\text{m}^2 \text{m}^{-2}$)	$\langle \text{TSI}_h \rangle$ (m)	Number of zones
1	30.6	143.1	1791.3	11.3	8.59	8.2	11
2	34.4	265.1	1804.3	10.2	9.02	7.26	12
3	64.7	111.1	1896.4	12.8	9.17	8.11	10
4	21.0	264.4	1834.1	9.3	9.13	6.67	4
5	11.6	98.3	1917.0	13.6	8.98	7.69	9
6	1.9	159.2	1864.9	15.0	8.92	8.63	3
7	30.1	91.6	2041.3	10.2	9.11	7.47	11
8	24.5	187.5	2063.9	11.2	10.57	6.83	12
9	82.7	133.3	2108.7	15.5	8.53	7.12	15
10	43.7	219.8	2074.8	13.7	8.43	7.08	15
12	2.7	293.3	1851.1	9.6	7.89	6.87	3
13	159.2	119.6	2060.7	16.8	7.46	7.13	18
14	92.2	238.6	2091.8	18.6	8.77	6.99	19
15	7.9	206.9	1880.2	3.2	7.75	10.6	3
16	67.9	283.7	1958.0	12.7	8.65	7.59	12
17	42.7	140.0	2130.7	19.3	6.50	6.57	17
18	54.1	229.3	2144.2	18.3	7.29	6.71	18
19	6.8	182.6	1972.8	11.9	5.82	7.93	4
20	34.8	284.4	2052.2	15.0	8.30	7.2	11
21	76.7	200.3	2229.5	19.4	6.23	6.6	17
22	21.4	274.4	2257.7	21.5	4.20	6.46	20
23	43.6	237.2	2185.4	18.5	6.21	6.72	20
24	57.4	300.7	2214.6	20.7	5.31	6.23	18
25	123.1	203.9	1993.3	9.9	9.23	7.64	21
26	195.5	276.5	2112.2	12.9	8.46	7.64	22

4. Results

Three sets of simulations were run with different parameter combinations. Following Mackay et al. (2003), an initial set of 2000 simulations were run for each of the 25 hillslopes with values for three canopy conductance parameters, g_{Smax} (range 17–126 $\text{mmol m}^{-2} \text{s}^{-1}$), Q_{min} (range 3000–9000 $\text{kJ m}^{-2} \text{day}^{-1}$), and δ (range 0.07–0.74 kPa^{-1}) randomly sampled from a naive (uniform) distribution. For this first set of simulations no parameters controlling available soil water were adjusted. Table 3 summarizes the average of these parameters taken from the ensemble of models retained using $|U(r) - \log_2 k|$ for the respective July and August TMS scenes. The Q_{min} averages are generally higher for August than for July, but no such clear pattern exists for g_{Smax} or δ . This indicates that there is a need for greater reduction in stomatal conductance for the August date

in comparison to July, and this reduction is not satisfied with a reduction in either g_{Smax} or δ . This is further evident in Fig. 4, which shows how stomatal sensitivity to D versus reference conductance for each hillslope compares to the theoretical universal line (Refer to Fig. 1) of stomatal regulation of leaf water potential (Oren et al., 1999). The figure clearly shows that the simulations for July are closely following the universal line. However, the simulations for August show considerable scatter, indicating that the simulation model is performing poorly when judged against the plant water-relations theory.

One hypothesis for the poor model performance for August is that soil moisture limitation is not adequately simulated. This reasoning would make sense if hillslopes at low elevation, with south-facing aspects and high leaf area index tended to follow the universal line the least. Fig. 5 shows a relationship between the calculated slope (m/G_{Sref}) and leaf area

Table 3

Summary of ensemble averages for the respective parameters for calibration with the July and August TMS images, respectively

Hillslope identifier	July			August		
	$E(Q_{min})$ ($\text{kJ m}^{-2} \text{day}^{-1}$)	$E(G_{Smax})$ ($\text{mmol m}^{-2} \text{s}^{-1}$)	$E(\delta)$ (kPa^{-1})	$E(Q_{min})$ ($\text{kJ m}^{-2} \text{day}^{-1}$)	$E(G_{Smax})$ ($\text{mmol m}^{-2} \text{s}^{-1}$)	$E(\delta)$ (kPa^{-1})
1	6565.0	85.8	0.433	5449.6	99.1	0.540
2	5641.0	73.8	0.410	5827.2	72.0	0.401
3	6305.2	80.0	0.411	7182.0	74.4	0.466
4	5639.8	75.9	0.420	6269.5	71.9	0.489
5	5892.9	73.2	0.389	6086.8	72.4	0.465
6	4890.0	43.9	0.359	5055.3	89.3	0.411
7	5823.0	68.6	0.428	7221.1	75.7	0.452
8	3588.6	61.0	0.406	5630.6	82.0	0.409
9	6689.6	67.4	0.433	6376.3	88.0	0.421
10	5798.1	71.3	0.403	6866.2	102.3	0.384
12	6655.6	61.4	0.442	3809.2	81.5	0.305
13	3561.4	41.9	0.413	7721.5	80.0	0.454
14	4910.7	54.8	0.442	7631.9	81.0	0.516
15	4112.3	60.7	0.411	5207.2	65.2	0.348
16	6006.6	80.8	0.402	6891.3	81.0	0.447
17	5503.4	69.1	0.412	5748.1	64.2	0.412
18	5558.6	71.4	0.417	5288.4	65.2	0.397
19	4738.1	44.6	0.413	4923.1	76.7	0.349
20	3460.6	66.8	0.406	3798.1	75.8	0.391
21	5353.8	81.2	0.432	5094.9	71.3	0.439
22	5475.0	84.6	0.396	5508.0	84.6	0.410
23	5451.5	77.1	0.394	5233.5	66.5	0.394
24	5371.6	81.9	0.416	5537.8	83.8	0.402
25	4010.8	43.5	0.420	6989.5	71.7	0.497
26	3917.9	59.3	0.415	6842.6	75.0	0.449

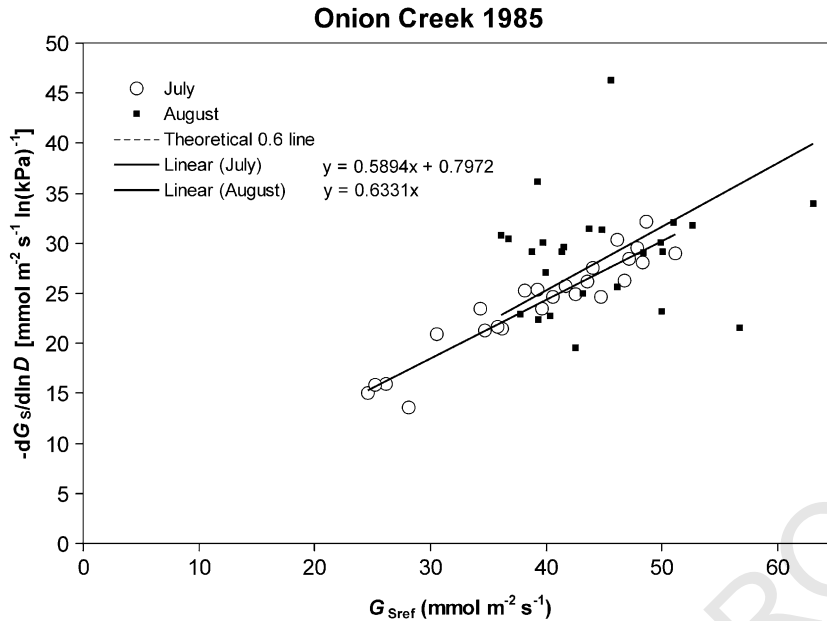


Fig. 4. These plots show the relationships between stomatal sensitivity to vapor pressure deficit and reference conductance at a vapor pressure deficit of 1 kPa for all hillslopes for both July and August TMS scene dates. The dashed line has a slope $0.6 \ln(\text{kPa})^{-1}$, which has been shown by a large volume of data and modeling to represent a universal tradeoff in stomatal function (Oren et al., 1999; Ewers et al., 2000). Plants that regulate their water potential to just prevent runaway cavitation should theoretically fall on this line. The solid lines represent linear regressions for the July and August points, respectively. For the August plots the regression line was forced through the origin, since we expect stomatal sensitivity to be zero at full stomatal closure. Note that both fitted lines have slope near the theoretical 0.6 line, and in particular the July result shows a strong fit ($R^2 = 0.89$).

index, L , for the hillslopes organized into three groups by elevation. At low elevation, high evaporative demand, sites there is a strong positive relationship between the m/G_{Sref} and L . This relationship is weaker at the intermediate elevations and non-existent at the high elevations. Where m/G_{Sref} is near 0.6 indicates that the simulations are consistent with the universal line. When m/G_{Sref} exceeds 0.6 this indicates δ is increasing to compensate for an underestimated soil moisture stress or too low Q_{min} . At values below 0.6 it is possible that simulated soil moisture stress is too great. While this result supports the notion that soil moisture limits are poorly represented in the simulations, it does not fully explain why Q_{min} increases for August. Fig. 6 shows a positive relationship between m/G_{Sref} and Q_{min} . In addition, the position of each hillslope (above or below $m/G_{Sref} = 0.6$) can be explained in terms of properties that affect water supply versus demand. Lower elevation hillslopes and a steep, southwest aspect hillslope have $m/G_{Sref} \gg 0.6$ and correspondingly higher Q_{min} . This indicates that

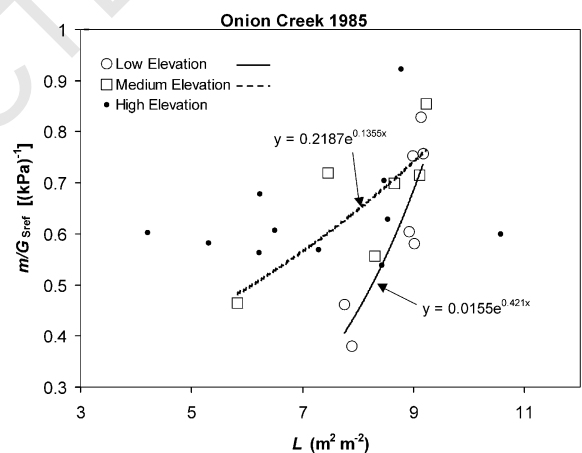


Fig. 5. Shown in this figure are relations between m/G_{Sref} , which theory suggests should have a value of 0.6, and leaf area index (L). The hillslopes have been sorted by their average elevation into low, medium and high categories to show that at lower elevations where temperatures are higher there is a relatively strong correspondence between the m/G_{Sref} and L . This relationship is not significant at the high elevations at which most of the hillslopes follow the theory.

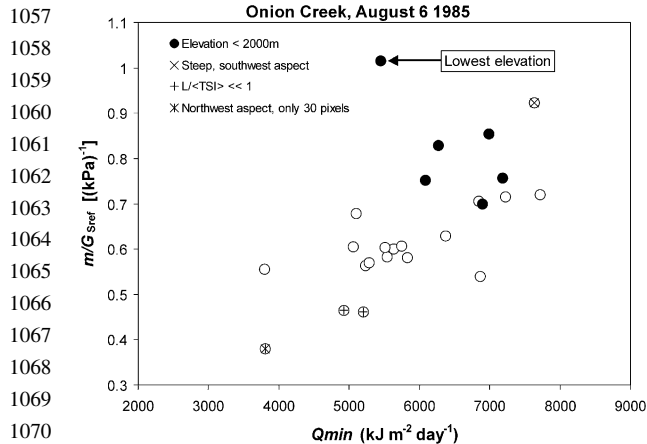


Fig. 6. Shown in this figure are relations between m/G_{Sref} , which theory suggests should have a value of 0.6, and Q_{min} . It shows a clear positive relationship that suggests that Q_{min} is compensating for factors controlling stomata that are not represented properly in the model, such as pre-dawn soil water potential. Individual hillslopes and groups of hillslopes, which do not follow water regulation theory ($m/G_{Sref} = 0.6$) are distinguished in terms of low elevation or high radiation load (steep, southwest aspect) for greater than expected apparent stomatal regulation of water potential, and low moisture demand versus supply ($L/\langle TSI \rangle \ll 1$) or northwest aspect for lower than expected apparent stomatal regulation of water potential.

areas of higher moisture demand for the amount of supply are simulated as too wet, which forces the canopy parameters to compensate by exceeding the universal line. Hillslopes with low L per unit $\langle TSI_h \rangle$ (an index of water demand versus supply) or northwest aspect have $m/G_{Sref} \ll 0.6$ and lower Q_{min} values. These hillslopes are simulated as having too little soil moisture, which requires the canopy parameters to compensate by falling below the universal line.

It appears that Q_{min} is being used incorrectly to compensate for a poor representation of soil water limitation on stomatal conductance. Since it is a surrogate for the light limitation on stomatal opening, which is species dependent, there is no clear justification for changing Q_{min} between July and August. To remedy this a second set of 2000 simulations per hillslope was run using a single Q_{min} of $5237 \text{ kJ m}^{-2} \text{ day}^{-1}$ determined as the average July Q_{min} for all hillslopes, and the rooting length parameter, R'_h , was randomly sampled from an uninformed distribution with a range of 0.01–0.1 m.

The results are shown in Fig. 7. Overall, there is a substantial improvement in the fit of each hillslope to the universal line for both dates. The August date still shows more scatter. Based on the inset plot in Fig. 7 there is a strong, positive relationship between m/G_{Sref} and the rooting length. This relationship is similar to the one shown in Fig. 6, indicating a tradeoff is occurring between R'_h and Q_{min} . To test this hypothesis, a third and final set of 2000 simulations was run using the ensemble average July Q_{min} values from Table 3, for the respective hillslopes. The results are shown in Fig. 8. The results show a tight clustering of all hillslopes on the universal line, but at a narrow range of G_{Sref} . Furthermore, R'_h , shown inset in Fig. 8, now has a narrow range of values, which means all hillslopes are converging to a point in parameter space.

5. Discussion

The parameter tradeoffs (g_{Smax} versus δ) seen in the daily simulations of transpiration suggest that the Jarvis model captures stomatal regulation of water potential. The tradeoffs seen with this relatively coarse simulation with sparse data are consistent with those proposed in theory (Monteith, 1995), extensively tested against a large amount of porometry and sap flux data (Oren et al., 1999), and obtained using a half-hourly model driven by in situ micrometeorology and calibrated with sap flux data (Mackay et al., 2003). It is important to realize that, without this direct comparison to water-relations theory, it is possible that numerous factors would have contributed to this apparent physically consistent behavior of the model. For example, there are abundant degrees of freedom given the uncertainties in both model inputs and in deriving surface temperature from TMS. Furthermore, one should be cautious in interpreting simulation model parameters obtained from ensemble averages. The values for the respective parameters may simply approach the mean of the a priori distributions from which they are sampled. This problem can be avoided by applying an iterative refinement of the parameter values, as was done in this paper. The fact that a large range of G_{Sref} is obtained for the first and second set of simulations (Figs. 4 and 7) is proof that parameter values for each

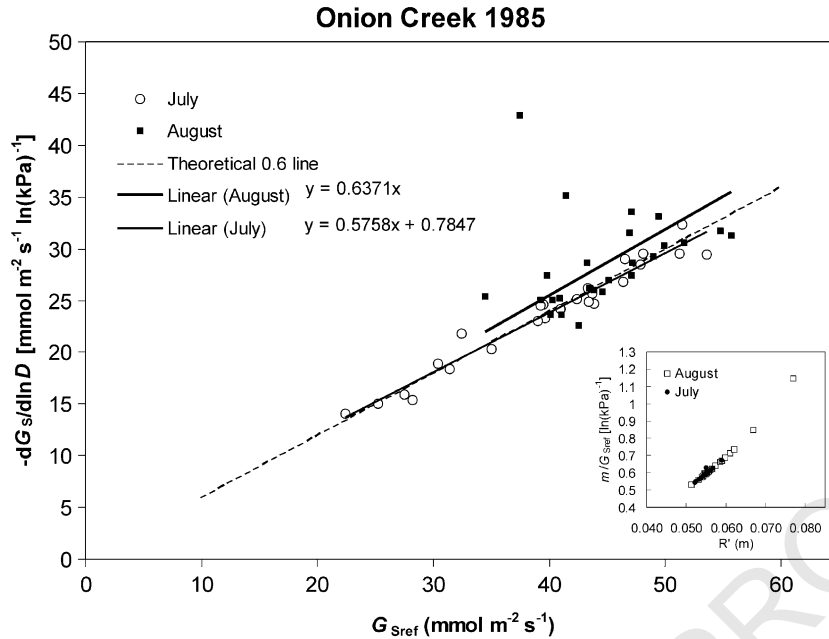


Fig. 7. These plots show the relationships between stomatal sensitivity to vapor pressure deficit and reference conductance at a vapor pressure deficit of 1 kPa for all hillslopes for both July and August TMS scene dates. This result is from the second set of simulations in which the rooting length scalar, R' , is varied. The dashed line has a slope $0.6 \ln(\text{kPa})^{-1}$, which has been shown by a large volume of data and modeling to represent a universal tradeoff in stomatal function (Oren et al., 1999; Ewers et al., 2000). Plants that regulate their water potential to just prevent runaway cavitation should theoretically fall on this line. The solid lines represent linear regressions for the July and August points, respectively. For the August plots the regression line was forced through the origin, since we expect stomatal sensitivity to be zero at full stomatal closure. Note that both fitted lines have slope near the theoretical 0.6 line, and in particular the July result shows a strong fit ($R^2 = 0.95$). August has a good fit for all except two hillslopes. Inset plots show relationships between m/G_{Sref} and the rooting length scalar.

hillslope are not simply taking on the distribution means for the respective parameters. Instead, the results show that by following water-relations theory a progressive refinement of the Jarvis-type model parameters is obtained.

The progressive refinement of model parameter values demonstrates an important distinction between automated versus knowledge-based parameterization schemes. Automated schemes (Binley and Beven, 1991; Gupta et al., 1998; Samanta and Mackay, 2003) tend to be naïve and extremely sensitive to the type of objective functions used, as would be the case in the present paper. Knowledge-based schemes are sensitive to the application domain (Franks and Beven, 1997; Boyle et al., 2000; Mackay et al., 2003), take into consideration intuition about the function of the modeled system, and tend to be less sensitive to specific objective functions. The universal line (Oren et al., 1999) summarizes a large amount of data on

plant hydraulic function. Based on the results in this paper for watershed-scale modeling and those of Mackay et al. (2003) for stand-level modeling, there is sufficient justification for argument that the Jarvis model parameters can be made to follow the universal line. This does not confirm that the models mimic plant hydraulic function, anymore than it confirms a direct correspondence between predicted stomatal conductance rates and what might be observed through more direct methods, such as sap flux. It does suggest the hypothesis that the combination of simulation model and thermal remote sensing data used in this paper with the particular data set is sensitive to the same tradeoffs in stomatal regulation of leaf water potential that is more directly quantifiable with sap flux. A study that combines ground validation, including sap flux, combined with thermal remote sensing data should be able to test this hypothesis.

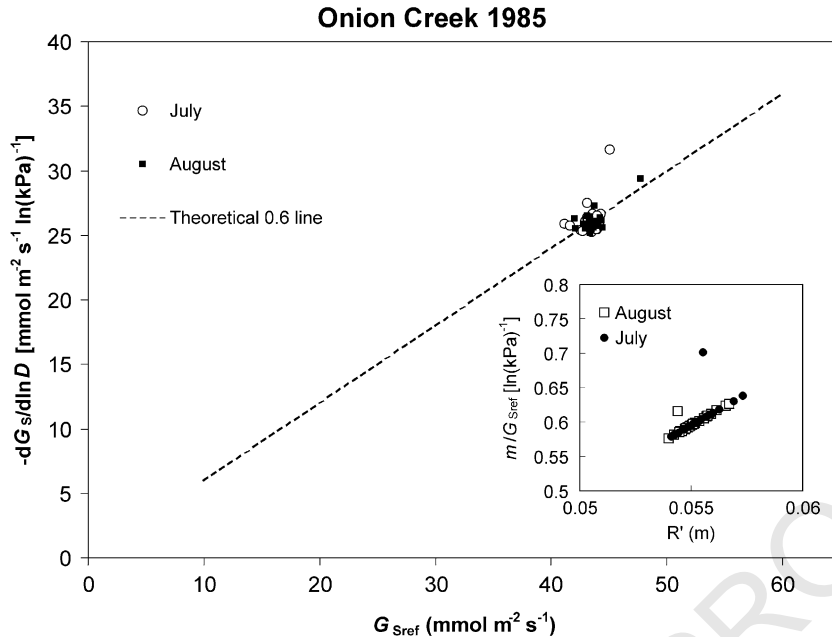


Fig. 8. These plots show the relationships between stomatal sensitivity to vapor pressure deficit and reference conductance at a vapor pressure deficit of 1 kPa for all hillslopes for both July and August TMS scene dates. This result is from the third set of simulations in which the rooting length scalar, R' , is varied, and Q_{\min} is derived from the July ensembles for the first set of simulations. The dashed line has a slope $0.6 \ln(\text{kPa})^{-1}$, which has been shown by a large volume of data and modeling to represent a universal tradeoff in stomatal function (Oren et al., 1999; Ewers et al., 2000). Plants that regulate their water potential to just prevent runaway cavitation should theoretically fall on this line. Inset plots show relationships between m/G_{Sref} and the rooting length scalar.

The results suggest that the four parameters, g_{Smax} , δ , Q_{\min} , and R'_h are sufficient for parameterizing the Jarvis model within RHESSys applied to conifer-covered watersheds. Among hillslope variations in Q_{\min} rooting depths or some similar proxy of available soil moisture appear to explain much of the variation among hillslopes. Once these are accounted for, g_{Smax} and δ parameters can be identified and are nearly equal for all hillslopes. While this is not necessarily representative of individual locations within the watershed, the average values of maximum stomatal conductance obtained are typical for conifer canopies (Running and Coughlan, 1988; Kelliher et al., 1995). This suggests that, at a scale of hillslopes or larger, average canopy parameters are acceptable, at least for the conifer biome. While this approach used to calibrate RHESSys does not resolve within-hillslope details in canopy parameters, it does allow for an assessment of physically meaningful parameter tradeoffs. The tradeoffs between canopy parameters indicate a physiological basis for interpreting

simulated transpiration. Based on the universal line transpiration rates are reduced either by lowering G_{Sref} or by increasing m . To prevent runaway cavitation a plant either needs to have a low set point for its leaf water potential, which requires a high structural integrity of its cell walls (or low vulnerability to cavitation), or it must safeguard against high leaf water potentials by closing stomata. On one hand, the 'efficiency' associated with a high G_{Sref} comes at a cost, as high K_L per unit L is needed to meet the high demand for water, and this makes the plant vulnerable to hydraulic failure (Ewers et al., 2000). On the other hand, the 'safety' associated with a low G_{Sref} means the plant can have a lower K_L per unit L . While this reduces its vulnerability to hydraulic failure when water is limiting or atmospheric demand for water is high it also compromises the photosynthetic capacity when water supply exceeds demand. This has direct implications for carbon gain and plant growth. The simulation model mimics this by either reducing g_{Smax} or increasing δ . A higher g_{Smax} allows a simulated

1345 plant to take advantage of optimal environmental
 1346 conditions to maximize CO₂ gain. These differences
 1347 in stomatal response to environmental factors have
 1348 important implications for land surface process
 1349 modeling of water and carbon exchange, from short
 1350 to long timescales. The safety versus efficiency
 1351 tradeoffs embodied provides a direct physical con-
 1352 nection between model parameterization and the
 1353 physiological functioning of vegetation at watershed
 1354 scales. As such, this model could be considered
 1355 complimentary to the traditional land surface para-
 1356 meterization schemes based on biome classification
 1357 coupled with remote sensing (Running et al., 1995;
 1358 Sellers et al., 1996; Zeng et al., 2000). Parameteriza-
 1359 tion of the variability in canopy physiology at large
 1360 scales then amounts to mapping the land surface into
 1361 positions along the continuum between safe and
 1362 efficient strategies. This could greatly simplify the
 1363 task of quantifying surface resistances over large
 1364 regions.

1365 A major challenge in parameterizing surface
 1366 resistance parameters from remote sensing is the
 1367 typical low signal-to-noise ratio. This has lead to the
 1368 use of thermal inertia (Anderson et al., 1997; Norman
 1369 et al., 2000) and empirical relations between veg-
 1370 etation vigor and surface temperature (Nemani and
 1371 Running, 1989; Carlson et al., 1995) to effectively
 1372 separate information from noise. The approach in this
 1373 paper is similar in that an empirical relationship
 1374 between reference conductance and stomatal sensi-
 1375 tivity to water loss is used to distinguish between
 1376 signal and noise. The approach is similar to that of
 1377 Franks and Beven (1997) in that spatial variation in
 1378 surface temperature is used to constrain the identifi-
 1379 cation of model parameters. A physical interpretation
 1380 in this paper relies on strong gradients in vegetation
 1381 types (grass versus gallery forest). The present paper
 1382 takes this type of analysis a significant step towards
 1383 finding a direct physical interpretation of parameters
 1384 in terms of the hydraulic functioning of the veg-
 1385 etation. This can resolve gradients in physiological
 1386 functioning even when taxonomic classification is
 1387 highly aggregated, as is typically the case for remote
 1388 sensing data. The results suggest a potential refine-
 1389 ment of current remote sensing algorithms to include
 1390 the universal line describing the regulation of leaf
 1391 water potential. This would improve future estimates
 1392 of land surface parameters, particularly for forests

1393 where strong gradients in surface temperature do not
 1394 necessarily accompany strong gradients in water flux.
 1395

1396 6. Conclusions

1397
 1398 A Jarvis-type model of stomatal conductance can
 1399 be reliably parameterized at a daily time scale in a
 1400 meso-scale watershed with a limited amount of
 1401 thermal remote sensing imagery. However, parameter
 1402 values need to be determined carefully, as there are
 1403 numerous compensations among parameters. The key
 1404 strength of the approach applied in this paper is that
 1405 parameter values are not chosen strictly based on
 1406 degree of fit between the simulated latent heat fluxes
 1407 and the surface temperatures obtained from the
 1408 thermal remote sensing data. Instead, a set of
 1409 simulation results that cannot be rejected based on
 1410 their information content is used as an ensemble.
 1411 Furthermore, the ensemble parameter values are
 1412 compared against water-relations theory, which
 1413 lends a direct physical interpretation to the estimated
 1414 parameters. The results are in agreement with those
 1415 obtained in other studies of direct analysis of leaf-
 1416 level porometry measurements, whole-tree sap flux
 1417 measurements, and whole canopy modeling validated
 1418 with sap flux measurements. While further work is
 1419 needed to assess the reliability of the approach across
 1420 a range of biomes, it appears to provide a direct link
 1421 between estimating stomatal conductance from
 1422 remote sensing data and more direct ground obser-
 1423 vations of plant water-relations.
 1424

1425 Acknowledgements

1426
 1427 This research was funded primarily by grants from
 1428 the NASA Land Surface Hydrology Program (NAG5-
 1429 8554), NASA Centers of Excellence in Remote
 1430 Sensing (NAG5-6535), USDA CSREES Hatch, and
 1431 the Wisconsin Alumni Research Foundation to DSM
 1432 Funding by the NASA Terrestrial Ecology Program to
 1433 LEB and RRN are acknowledge for developments of
 1434 RHESSys and data collection from Onion Creek. We
 1435 are grateful to Lars Pierce and Lee MacDonald who
 1436 collected the Onion Creek data in 1985. We thank
 1437 Brent Ewers for comments on an earlier draft, and two
 1438 anonymous reviewers whose comments have lead to
 1439 substantial improvements, of the manuscript.
 1440

References

- 1441 Aber, J.D., Federer, C.A., 1992. A generalized, lumped-parameter
1442 model of photosynthesis, evapotranspiration and net primary
1443 production in temperate and boreal forest ecosystems. *Oecologia* 92, 463–474.
1444
1445 Anderson, M.C., Norman, J.M., Diak, G.R., Kustas, W.P., 1997. A
1446 two-source integrated model for estimating surface fluxes for
1447 thermal infrared satellite observations. *Remote Sensing of*
1448 *Environment* 60, 195–216.
1449
1450 Ball, J.T., Woodrow, I.E., Berry, J.A., 1987. A model predicting
1451 stomatal conductance and its contribution to the control of
1452 photosynthesis under different environmental conditions. In:
1453 Biggens, J., (Ed.), *Progress in Photosynthesis Research*, vol. 4.
1454 Martinus Nijhoff Publishers, Dordrecht, the Netherlands,
1455 pp. 221–229.
1456
1457 Band, L.E., Patterson, P., Nemani, R., Running, S.W., 1993. Forest
1458 ecosystem processes at the watershed scale: incorporating
1459 hillslope hydrology. *Agricultural and Forest Meteorology* 63,
1460 93–126.
1461
1462 Band, L.E., Mackay, D.S., Creed, I., Semkin, R., Jeffries, D.S.,
1463 1996. Ecosystem processes at the watershed scale: sensitivity to
1464 potential climate change. *Limnology and Oceanography* 41 (5),
1465 928–938.
1466
1467 Baron, J.S., Hartman, M.D., Band, L.E., Lammers, R.B., 2000.
1468 Sensitivity of a high elevation Rocky Mountain watershed to
1469 altered climate and CO₂. *Water Resources Research* 36 (1),
1470 89–99.
1471
1472 Bastiaanssen, W.G.M., Menenti, M., Feddes, R.A., Holtslag,
1473 A.A.M., 1998. A remote sensing surface energy balance
1474 algorithm for land (SEBAL). 1. Formulation. *Journal of*
1475 *Hydrology* 212/213, 198–212.
1476
1477 Beven, K., 1986. Runoff production and flood frequency in
1478 catchments of order *n*: an alternative approach. In: Gupta,
1479 V.K., Rodriguez-Iturbe, I., Wood, E.F. (Eds.), *Scale Problems in*
1480 *Hydrology*, D. Reidel Publishing Co, Dordrecht, pp. 107–131.
1481
1482 Beven, K.J., Binley, A., 1992. The future of distributed models:
1483 model calibration and uncertainty prediction. *Hydrological*
1484 *Processes* 6, 279–298.
1485
1486 Beven, K.J., Kirkby, M.J., 1979. A physically based, variable
1487 contributing area model of basin hydrology. *Hydrological*
1488 *Sciences Bulletin* 1, 43–69.
1489
1490 Binley, A.M., Beven, K.J., 1991. Physically-based modeling of
1491 catchment hydrology: a likelihood approach to reducing
1492 predictive uncertainty. In: Farmer, D.J., Rycroft, M.J. (Eds.),
1493 *Computer Modelling in the Environmental Sciences*, IMA
1494 *Conference Series*. Clarendon Press, Oxford, pp. 75–88.
1495
1496 Boyle, D.P., Gupta, H.V., Sorooshian, S., 2000. Toward improved
1497 calibration of hydrologic models: combining the strengths of
1498 manual and automated methods. *Water Resources Research* 36
1499 (12), 3663–3674.
1500
1501 Brooks, R.H., Corey, A.T., 1964. *Hydraulic Properties of Porous*
1502 *Media*, Hydrologic Paper 3, Colorado State University, Fort
1503 Collins, p. 27.
1504
1505 Carlson, T.N., Capehart, W.J., Gillies, R.R., 1995. A new look at the
1506 simplified method for remote sensing of daily evapotranspira-
1507 tion. *Remote Sensing of Environment* 54, 161–167.
1508
1509 Crago, R.D., 1996. Conservation and variability of the evaporative
1510 fraction during the daytime. *Journal of Hydrology* 180,
1511 173–194.
1512
1513 Crago, R.D., Brutsaert, W., 1996. Daytime evaporation and self-
1514 preservation of the evaporative fraction and the Bowen ratio.
1515 *Journal of Hydrology* 178, 241–255.
1516
1517 Creed, I.F., Band, L.E., Foster, N.W., Morrison, I.K., Nicolson,
1518 J.A., Semkin, R.S., Jeffries, D.S., 1996. Regulation of nitrate-N
1519 release from temperate forests: a test of the N flushing
1520 hypothesis. *Water Resources Research* 32 (11), 3337–3354.
1521
1522 Ewers, B.E., Oren, R., Sperry, J.S., 2000. Influence of nutrient
1523 versus water supply on hydraulic architecture and water balance
1524 in *Pinus taeda*. *Plant, Cell and Environment* 23, 1055–1066.
1525
1526 Ewers, B.E., Oren, R., Johnsen, K.H., Landsberg, J.J., 2001.
1527 Estimating maximum mean canopy stomatal conductance for
1528 use in models. *Canadian Journal of Forest Research* 31, 198–207.
1529
1530 Famiglietti, J.S., Wood, E.F., 1994. Multi-scale modeling of
1531 spatially-variable water and energy balance processes. *Water*
1532 *Resources Research* 30, 3061–3078.
1533
1534 Foley, J.A., Prentice, I.C., Ramankutty, N., Levis, S., Pollard, D.,
1535 Sitch, S., Haxeltine, A., 1996. An integrated biosphere model of
1536 land surface processes, terrestrial carbon balance, and veg-
1537 etation dynamics. *Global Biogeochemical Cycles* 10 (4),
1538 603–628.
1539
1540 Foley, J.A., Levis, S., Costa, M.H., Cramer, W., Pollard, D., 2000.
1541 Incorporating dynamic vegetation cover within global climate
1542 models. *Ecological Applications* 10 (6), 1620–1632.
1543
1544 Franks, S., Beven, K.J., 1997. Estimation of evapotranspiration at
1545 the landscape scale: a fuzzy disaggregation approach. *Water*
1546 *Resources Research* 33 (12), 2929–2938.
1547
1548 van Genuchten, M.Th., 1980. A closed-form equation for predicting
1549 the hydraulic conductivity of unsaturated soils. *Soils Science*
1550 *Society of America Journal* 44, 892–898.
1551
1552 Gholtz, H.L., 1982. Environmental limits on aboveground net
1553 primary production, leaf area, and biomass in vegetation zones
1554 of the pacific northwest. *Ecology* 63 (2), 469–481.
1555
1556 Goward, S.N., Cruickshanks, G.D., Hope, A.S., 1985. Observed
1557 relation between thermal emission and reflected spectral
1558 radiance of a complex vegetation landscape. *Remote Sensing*
1559 *of Environment* 18, 137–146.
1560
1561 Grier, C.C., Running, S.W., 1977. Leaf area of mature northwestern
1562 coniferous forests: relation to site water balance. *Ecology* 58,
1563 893–899.
1564
1565 Gupta, H.V., Sorooshian, S., Yapo, P.O., 1998. Towards improved
1566 calibration of hydrologic models: multiple and non-commensur-
1567 able measures of information. *Water Resources Research* 34 (4),
1568 751–763.
1569
1570 Hartley, R.V.L., 1928. Transmission of information. *The Bell*
1571 *Systems Technical Journal* 7 (3), 535–563.
1572
1573 Higashi, M., Klir, G.J., 1982. On measures of fuzziness and fuzzy
1574 complements. *International Journal of General Systems* 8 (3),
1575 169–180.
1576
1577 Holbo, H.R., Luvall, J.C., 1989. Modeling surface temperature
1578 distributions in forest landscapes. *Remote Sensing of Environ-*
1579 *ment* 27, 11–24.
1580
1581 Idso, S.B., Reginato, R.J., Jackson, R.D., 1978. An equation for
1582 potential evaporation from soil, water and crop surfaces
1583 1584 1585 1586 1587 1588 1589 1590 1591 1592 1593 1594 1595 1596

- 1537 adaptable to use by remote sensing. *Geophysical Research*
 1538 *Letters* 4, 187–188.
- 1539 Jackson, R.D., Idso, S.B., Reginato, R.J., Pinter, P.J. Jr., 1981.
 1540 Canopy temperature as a crop water stress indicator. *Water*
 1541 *Resources Research* 17, 1133–1138.
- 1542 Jarvis, P.G., 1976. The interpretation of the variations in leaf water
 1543 potential and stomatal conductance found in canopies in the
 1544 field. *Philosophical Transactions of the Royal Society of*
 1545 *London, Series B* 273, 593–610.
- 1546 Jarvis, P.G., 1980. Stomatal response to water stress in conifers. In:
 1547 Turner, N.C., Kramer, P.J. (Eds.), *Adaptation of Plants to Water*
 1548 *and High Temperature Stress*, Wiley, New York, pp. 105–122.
- 1549 Kelliher, F.M., Leuning, R., Raupach, M.R., Schulze, E.-D., 1995.
 1550 Maximum conductances for evaporation from global vegetation
 1551 types. *Agricultural and Forest Meteorology* 73, 1–16.
- 1552 Klepper, O., Scholten, H., Van De Kamer, J.P.G., 1991. Prediction
 1553 uncertainty in an ecological model of the Oosterschelde Estuary.
 1554 *Journal of Forecasting* 10, 191–209.
- 1555 Klir, G.J., Wierman, M.J., 1998. *Uncertainty-Based Information:*
 1556 *Elements of Generalized Information Theory*, Physica-Verlag,
 1557 Heidelberg.
- 1558 Kuczera, G., 1982. On the relationship between the reliability of
 1559 parameter estimates and hydrologic time series data used in
 1560 calibration. *Water Resources Research* 18 (1), 146–154.
- 1561 Kuczera, G., 1983. Improved parameter inference in catchment
 1562 models. 2. Combining different kinds of hydrologic data and
 1563 testing their compatibility. *Water Resources Research* 19 (5),
 1564 1163–1172.
- 1565 Kuczera, G., Parent, E., 1998. Monte Carlo assessment of parameter
 1566 uncertainty in conceptual catchment models: the Metropolis
 1567 algorithm. *Journal of Hydrology* 211, 69–85.
- 1568 Kustas, W.P., Perry, E.M., Doraiswamy, P.C., Moran, M.S., 1994.
 1569 Using satellite remote sensing to extrapolate evapotranspiration
 1570 estimates in time and space over a semiarid rangeland basin.
 1571 *Remote Sensing of Environment* 49, 275–286.
- 1572 Larcher, W., 1995. *Physiological Plant Ecology*, 3rd ed, Springer,
 1573 Berlin.
- 1574 Leuning, R., Kelliher, F.M., De Pury, D.G.G., Schulze, E.-D., 1995.
 1575 Leaf nitrogen, photosynthesis, conductance and transpiration:
 1576 scaling from leaves to canopies. *Plant, Cell and Environment*
 1577 18, 1183–1200.
- 1578 Liang, C., Mackay, D.S., 2000. A general model of watershed
 1579 extraction and representation using globally optimal flow paths
 1580 and up-slope contributing areas. *International Journal of*
 1581 *Geographical Information Science* 14 (4), 337–358.
- 1582 Lohammar, T., Larsson, S., Linder, S., Falk, S.O., 1980. FAST-
 1583 simulation models of gaseous exchange in Scots pine.
 1584 *Ecological Bulletin* 32, 505–523.
- 1585 MacDonald, L.H., 1986. Persistence of Soil Moisture Changes
 1586 Resulting from Artificially Extended Snowmelt, *Proceedings of*
 1587 *the Western Snow Conference*, Phoenix, AZ, April 15–17,
 1588 1985, Colorado State University Press, Fort Collins,
 1589 pp. 146–149.
- 1590 MacDonald, L.H., 1987. Forest harvest, snowmelt and streamflow
 1591 in the Central Sierra Nevada. *Forest Hydrology and Watershed*
 1592 *Management (Proceedings of the Vancouver Symposium,*
 1593 *August, 1987)*, 273–283.
- 1594 MacDonald, L.H., 1989. *Snowmelt and Streamflow in the Central*
 1595 *Sierra Nevada: Effects of Forest Harvest and Cloud-Seeding.*
 1596 *Unpublished PhD Dissertation, Department of Forestry and*
 1597 *Resource Management, University of California, Berkeley.*
- 1598 Mackay, D.S., 2003. Evaluation of hydrologic equilibrium in a
 1599 mountainous watershed: incorporating forest canopy spatial
 1600 adjustment to soil biogeochemical processes. *Advances in*
 1601 *Water Resources in press.*
- 1602 Mackay, D.S., Band, L.E., 1997. Forest ecosystem processes at the
 1603 watershed scale: dynamic coupling of distributed hydrology and
 1604 canopy growth. *Hydrological Processes* 11, 1197–1217.
- 1605 Mackay, D.S., Robinson, V.B., 2000. A multiple criteria decision
 1606 support system for testing integrated environmental models.
 1607 *Fuzzy Sets and Systems* 113, 53–67.
- 1608 Mackay, D.S., Ahl, D.E., Ewers, B.E., Samanta, S., Gower, S.T.,
 1609 Burrows, S.N., 2003. Physiological tradeoffs in the parameter-
 1610 ization of a model of canopy transpiration. *Advances in Water*
 1611 *Resources in press.*
- 1612 McNaughton, K.G., Jarvis, P.G., 1991. Effects of spatial scale on
 1613 stomatal control of transpiration. *Agricultural and Forest*
 1614 *Meteorology* 54, 279–301.
- 1615 Melching, C.S., 1995. In: Singh, V.P., (Ed.), *Reliability Estimation*
 1616 *in Computer Models of Watershed Hydrology*, Water Resources
 1617 *Publication, Highlands Ranch, CO*, pp. 69–118.
- 1618 Monteith, J.L., 1965. *Evaporation and Environment*, *Proceedings of*
 1619 *the 19th Symposium of the Society for Experimental Biology*,
 1620 *Cambridge University Press, New York*, pp. 205–233.
- 1621 Monteith, J.L., 1995. A reinterpretation of stomatal response to
 1622 humidity. *Plant, Cell and Environment* 18, 357–364.
- 1623 Nemani, R.R., Running, S.W., 1989. Estimation of regional surface
 1624 resistance to evapotranspiration from NDVI and thermal-IR
 1625 AVHRR data. *Journal of Applied Meteorology* 28 (4),
 1626 276–284.
- 1627 Nemani, R., Pierce, L., Running, S., Band, L., 1993. Forest
 1628 ecosystem processes at the watershed scale: sensitivity to
 1629 remotely-sensed leaf area index estimates. *International Journal*
 1630 *of Remote Sensing* 14 (13), 2519–2534.
- 1631 Norman, J.M., Kustas, W.P., Prueger, J.H., Diak, G.R., 2000.
 1632 Surface flux estimation using radiometric temperature: a dual-
 1633 temperature-difference method to minimize measurement
 1634 errors. *Water Resources Research* 36 (8), 2263–2274.
- 1635 Oren, R., Sperry, J.S., Katul, G.G., Pataki, D.E., Ewers, B.E.,
 1636 Phillips, N., Schafer, K.V.R., 1999. Survey and synthesis of
 1637 intra- and interspecific variation in stomatal sensitivity to
 1638 vapour pressure deficit. *Plant, Cell and Environment* 22,
 1639 1515–1526.
- 1640 Oreskes, N., Shrader-Frechette, K., Belitz, K., 1994. Verification,
 1641 validation, and confirmation of numerical models in the earth
 1642 sciences. *Science* 263, 641–646.
- 1643 Pierce, L.L., Congalton, R.G., 1988. A methodology for mapping
 1644 forest latent heat flux densities using remote sensing. *Remote*
 1645 *Sensing of Environment* 24, 405–418.
- 1646 Quinn, P., Beven, K., Lamb, R., 1995. The $\ln(a/\tan B)$ index: how to
 1647 calculate it and how to use it within the TOPMODEL
 1648 framework. *Hydrological Processes* 9, 161–182.
- 1649 Running, S.W., Coughlan, J.C., 1988. A general model of forest
 1650 ecosystem processes for regional applications. I. Hydrologic

- 1633 balance, canopy gas exchange and primary production pro-
1634 cesses. *Ecological Modeling* 42, 125–154.
- 1635 Running, S.W., Hunt, E.R. Jr., 1993. Generalization of a forest
1636 ecosystem process model for other biomes, BIOME-BGC, and
1637 application for global scale models. In: Ehleringer, J.R., Field,
1638 C.B. (Eds.), *Scaling Physiological Processes: Leaf to Globe*,
1639 Academic Press, San Diego, CA, pp. 141–158.
- 1640 Running, S.W., Loveland, T.R., Pierce, L.L., Nemani, R.R., Hunt,
1641 E.R. Jr., 1995. A remote sensing based vegetation classification
1642 logic for global land cover analysis. *Remote Sensing of*
1643 *Environment* 51, 39–58.
- 1644 Saliendra, N.Z., Sperry, J.S., Comstock, J.P., 1995. Influence of leaf
1645 water status on stomatal response to humidity, hydraulic
1646 conductance, and soil drought in *Betula occidentalis*. *Planta*
1647 196, 357–366.
- 1648 Samanta, S., Mackay, D.S., 2003. Flexible automated parameter-
1649 ization of hydrologic models using fuzzy logic. *Water*
1650 *Resources Research* in press.
- 1651 Seguin, B., Itier, B., 1983. Using midday surface temperature to
1652 estimate daily evaporation from satellite thermal IR data.
1653 *International Journal of Remote Sensing* 4, 371–383.
- 1654 Sellers, P.J., Los, S.O., Tucker, C.J., Justice, C.O., Dazlich, D.A.,
1655 Collatz, G.J., Randall, D.A., 1996. A revised land surface
1656 parameterization (SiB₂) for atmospheric GCMs. Part II. The
1657 generation of global fields of terrestrial biophysical parameters
1658 from satellite data. *Journal of Climate* 9, 676–705.
- 1659 Sellers, P.J., Dickinson, R.E., Randall, D.A., et al., 1997. Modeling
1660 the exchange of energy, water, and carbon between continents
1661 and the atmosphere. *Science* 275, 502–509.
- 1662 Sivapalan, M., Beven, K., Wood, E.F., 1987. On hydrologic 2. A
1663 scaled model of storm runoff production. *Water Resources*
1664 *Research* 23, 2266–2278.
- 1665 Sorooshian, S., Gupta, V.K., 1983. Automatic calibration of
1666 conceptual rainfall–runoff models: the question of parameter
1667 observability and uniqueness. *Water Resources Research* 19 (1),
1668 251–259.
- 1669 Spear, R.C., Hornberger, G.M., 1990. Eutrophication in Peel Inlet—
1670 II identification of critical uncertainty via generalized sensitivity
1671 analysis. *Water Resources Research* 14, 43–49.
- 1672 Sperry, J.S., Adler, J.R., Campbell, G.S., Comstock, J.S., 1998.
1673 Hydraulic limitation of a flux and pressure in the soil–plant
1674 continuum: results from a model. *Plant, Cell and Environment*
1675 21, 347–359.
- 1676 van Stratten, G., Keesman, K.J., 1991. Uncertainty propagation and
1677 speculation in projective forecasts of environmental change:
1678 a lake-eutrophication example. *Journal of Forecasting* 10,
1679 163–190.
- 1680 Tague, C.L., Band, L.E., 2001. Evaluating explicit and implicit
1681 routing for watershed hydro-ecological models of forest
1682 hydrology at the small catchment scale. *Hydrological Processes*
1683 15, 1415–1439.
- 1684 Tyree, M.T., Ewers, F.E., 1991. The hydraulic architecture of trees
1685 and other woody plants. *New Phytologist* 119, 345–360.
- 1686 Tyree, M.T., Sperry, J.S., 1988. Do woody plants operate near the
1687 point of catastrophic xylem dysfunction caused by dynamic
1688 water stress? Answers from a model. *Plant Physiology* 88,
1689 574–580.
- 1690 Vertessy, R.A., Hatton, T.J., Benyon, R.G., Dawes, W.R., 1996.
1691 Long-term growth and water balance predictions for a mountain
1692 ash (*Eucalyptus regnans*) for catchment subject to clear-felling
1693 and regeneration. *Tree Physiology* 16, 221–232.
- 1694 Watson, G.R., Vertessy, R.A., Band, L.E., 1996. Distributed
1695 parameterization of a large scale water balance model for an
1696 Australian forested region. *HydroGIS 96: Application of*
1697 *Geographic Information Systems in Hydrology and Water*
1698 *Resources Management (Proceedings of Vienna Conference,*
1699 *April 1996)*, IAHS Publication No. 235.
- 1700 White, J.D., Running, S.W., Thornton, P.E., Keane, R.E., Ryan,
1701 K.C., Farge, D.B., Key, C.H., 1998. Assessing simulated
1702 ecosystem processes for climate variability research at Glacier
1703 National Park, USA. *Ecological Applications* 8 (3), 805–823.
- 1704 Wigmosta, M.S., Vail, L.W., Lettenmaier, D.P., 1994. A distributed
1705 hydrology-vegetation model for complex terrain. *Water*
1706 *Resources Research* 30 (6), 1665–1679.
- 1707 Yapo, P.O., Gupta, H.V., Sorooshian, S., 1998. Multi-objective
1708 global optimization for hydrologic models. *Journal of Hydrol-*
1709 *ogy* 204, 83–97.
- 1710 Yong, J.W.H., Wong, S.C., Farquhar, G.D., 1997. Stomatal
1711 response to changes in vapour pressure difference between
1712 leaf and air. *Plant, Cell and Environment* 20, 1213–1216.
- 1713 Zadeh, L.A., 1965. Fuzzy sets. *Information and Control* 8 (3),
1714 338–353.
- 1715 Zadeh, L.A., 1978. Fuzzy sets as a basis for a theory of possibilities.
1716 *International Journal of Fuzzy Sets and Systems* 1 (1), 3–28.
- 1717 Zeng, X., Dickinson, R.E., Walker, A., Shaikh, M., DeFries, R.S.,
1718 Qi, J., 2000. Derivation and evaluation of global 1-km fractional
1719 vegetation cover data for land modeling. *Journal of Applied*
1720 *Meteorology* 39, 826–839.
- 1721 Zhu, A.-X., Mackay, D.S., 2001. Effects of spatial detail of soil
1722 information on watershed modeling. *Journal of Hydrology* 248,
1723 54–77.